

# PyGeNN: A Python library for GPU-enhanced neural networks

James C Knight<sup>1,\*</sup>, Anton Komissarov<sup>2</sup>, Thomas Nowotny<sup>1</sup>

<sup>1</sup>Centre for Computational Neuroscience and Robotics, School of Engineering and Informatics, University of Sussex, Brighton, United Kingdom

<sup>2</sup>(**TODO: ANTON'S AFFILIATION**)

Correspondence\*:

James C Knight

J.C.Knight@sussex.ac.uk

## 2 ABSTRACT

More than half of the Top 10 supercomputing sites worldwide use GPU accelerators and they are becoming ubiquitous in workstations and edge computing devices. GeNN is a C++ library for generating efficient spiking neural network simulation code for GPUs. However, until now, the full flexibility of GeNN could only be harnessed by writing model descriptions and simulation code in C++. Here we present PyGeNN, a Python package which exposes all of GeNN's functionality to Python with minimal overhead. This provides an alternative, arguably more user-friendly, way of using GeNN and allows modellers to use GeNN within the growing Python-based machine learning and computational neuroscience ecosystems. In addition, we demonstrate that, in both Python and C++ GeNN simulations, the overheads of recording spiking data can strongly affect runtimes and show how a new spike recording system can reduce these overheads by up to 10×. Using the new recording system, we demonstrate that by using PyGeNN on a modern GPU, we can simulate a full-scale model of a cortical column faster even than real-time neuromorphic systems. Finally, we show that long simulations of a smaller model with complex stimuli and a custom three-factor learning rule defined in PyGeNN can be simulated up to 72× faster than real-time.

**Keywords:** GPU, high-performance computing, parallel computing, benchmarking, computational neuroscience, spiking neural networks, Python

## 1 INTRODUCTION

A wide range of spiking neural network (SNN) simulators are available, each with their own application domains. NEST (Gewaltig and Diesmann, 2007) is widely used for large-scale point neuron simulations on distributed computing systems; NEURON (Carnevale and Hines, 2006) and Arbor (Akar et al., 2019) specialise in the simulation of complex multi-compartmental models; NeuroKernel (Givon and Lazar, 2016) is focused on emulating fly brain circuits using Graphics Processing Units (GPUs); and CARLsim (Chou et al., 2018), ANNarchy (Vitay et al., 2015), NeuronGPU (Golosio et al., 2020) and GeNN (Yavuz et al., 2016) use GPUs to accelerate point neuron models. For performance reasons, many of these simulators are written in C++ and, especially amongst the older simulators, users describe their models either using a Domain-Specific Language (DSL) or directly in C++. For programming language purists, a DSL may be an elegant way of describing an SNN network model and, for simulator developers, not having to add bindings

to another language is convenient. However, both choices act as a barrier to potential users. Therefore, with both the computational neuroscience and machine learning communities gradually coalescing towards a Python-based ecosystem with a wealth of mature libraries for scientific computing (Hunter, 2007; Van Der Walt et al., 2011; Millman and Aivazis, 2011), exposing spiking neural network simulators to Python seems a pragmatic choice. NEST (Eppler et al., 2009), NEURON (Hines et al., 2009) and CARLsim (Balaji et al., 2020) have all taken this route and now all offer Python interfaces. Furthermore, newer simulators such as Arbor and Brian2 (Stimberg et al., 2019) have been designed from the ground up with a Python interface.

Our GeNN simulator can already be used as a backend for the Python-based Brian2 simulator (Stimberg et al., 2019) using the Brian2GeNN interface (Stimberg et al., 2020) which modifies the C++ backend “cpp\_standalone” of Brian 2 to generate C++ input files for GeNN. As for cpp\_standalone, initialisation of simulations is mostly done in C++ on the CPU and recording data is saved into binary files and re-imported into Python using Brian 2’s native methods. While we have recently demonstrated some very competitive performance results (Knight and Nowotny, 2018, 2020) using GeNN in C++, and through the Brian2GeNN interface (Stimberg et al., 2020), GeNN could so far not be used directly from Python and it is not possible to expose all of GeNN’s unique features through the Brian2 API. Specifically, GeNN not only allows users to easily define their own neuron and synapse models but, also ‘snippets’ for offloading the potentially costly initialisation of model parameters and connectivity onto the GPU. Additionally, GeNN provides a lot of freedom for users to integrate their own code into the simulation loop. In this paper we describe the implementation of PyGeNN – a Python package which aims to expose the full range of GeNN functionality with minimal performance overheads. Unlike in the majority of other SNN simulators PyGeNN allows defining bespoke neuron and synapse models directly from Python without requiring users to extend the underlying C++ code. Below, we demonstrate the flexibility and performance of PyGeNN in two scenarios where minimising performance overheads is particularly critical.

- In a simulation of a large, highly-connected model of a cortical microcircuit (Potjans and Diesmann, 2014) with small simulation timesteps. Here the cost of copying spike data off the GPU from a large number of neurons every timestep can become a bottleneck.
- In a simulation of a much smaller model of Pavlovian conditioning (Izhikevich, 2007) where learning occurs over 1 h of biological time and stimuli are delivered – following a complex scheme – throughout the simulation. Here any overheads are multiplied by a large number of timesteps and copying stimuli to the GPU can become a bottleneck.

Using the facilities provided by PyGeNN, we show that both scenarios can be simulated from Python with only minimal overheads over a pure C++ implementation.

## 2 MATERIALS AND METHODS

### 2.1 GeNN

GeNN (Yavuz et al., 2016) is a library for generating CUDA (NVIDIA et al., 2020) code for the simulation of spiking neural network models. GeNN handles much of the complexity of using CUDA directly and automatically performs device-specific optimizations so as to maximize performance. GeNN consists of a main library – implementing the API used to define models as well as the generic parts of the code generator – and an additional library for each backend (currently there is a reference C++ backend for generating CPU code and a CUDA backend. An OpenCL backend is under development). Users describe their model by implementing a `modelDefinition` function within a C++ file. For example, a model

consisting of 4 Izhikevich neurons with heterogeneous parameters, driven by a constant input current might be defined as follows:

```
72 void modelDefinition(ModelSpec &model)
73 {
74     model.setDT(0.1);
75     model.setName("izhikevich");
76
77     NeuronModels::IzhikevichVariable::VarValues popInit(
78         -65.0, -20.0, uninitialisedVar(), uninitialisedVar(),
79         uninitialisedVar(), uninitialisedVar());
80
81     model.addNeuronPopulation<NeuronModels::IzhikevichVariable>(
82         "Pop", 4, {}, popInit);
83
84     model.addCurrentSource<CurrentSourceModels::DC>(
85         "CS", "Pop", {10.0}, {});
86 }
```

The *genn-buildmodel* command line tool is then used to compile this file; link it against the main GeNN library and the desired backend library; and finally run the resultant executable to generate the source code required to build a simulation dynamic library (a .dll file on Windows or a .so file on Linux and Mac). This dynamic library can then either be statically linked against a simulation loop provided by the user or dynamically loaded by the user's simulation code. To demonstrate this latter approach, the following example uses the [SharedLibraryModel](#) helper class supplied with GeNN to dynamically load the previously defined model, initialise the heterogenous neuron parameters and print each neuron's membrane voltage every timestep:

```
95 #include "sharedLibraryModel.h"
96
97 int main()
98 {
99     SharedLibraryModel<float> model("./", "izhikevich");
100     model.allocateMem();
101     model.initialize();
102     float *aPop = model.getScalar<float>("aPop");
103     float *bPop = model.getScalar<float>("bPop");
104     float *cPop = model.getScalar<float>("cPop");
105     float *dPop = model.getScalar<float>("dPop");
106     aPop[0] = 0.02; bPop[0] = 0.2; cPop[0] = -65.0; dPop[0] = 8.0;
107     aPop[1] = 0.1; bPop[1] = 0.2; cPop[1] = -65.0; dPop[1] = 2.0;
108     aPop[2] = 0.02; bPop[2] = 0.2; cPop[2] = -50.0; dPop[2] = 2.0;
109     aPop[3] = 0.02; bPop[3] = 0.2; cPop[3] = -55.0; dPop[3] = 4.0;
110     model.initializeSparse();
111
112     float *vPop = model.getScalar<float>("VPop");
113     while(model.getTime() < 200.0f) {
114         model.stepTime();
115         model.pullVarFromDevice("Pop", "V");
116         printf("%f, %f, %f, %f, %f\n",
```

```

117         t, VPop[0], VPop[1], VPop[2], VPop[3]);
118     }
119     return EXIT_SUCCESS;
120 }

```

## 121 2.2 SWIG

122 In order to use GeNN from Python, both the model creation API and the `SharedLibraryModel`  
 123 functionality need to be ‘wrapped’ so they can be called from Python. While this is possible using  
 124 the API built into Python itself, wrapper functions would need to be manually implemented for each GeNN  
 125 function to be exposed which would result in a lot of maintenance overhead. Instead, we chose to use  
 126 SWIG (Beazley, 1996) to automatically generate wrapper functions and classes. SWIG generates Python  
 127 modules based on special interface files which can directly include C++ code as well as special ‘directives’  
 128 which control SWIG. For example, the following SWIG interface file would wrap the C++ code in `test.h` in  
 129 a Python module called `test_module` within a Python packages called `test_package`:

```

130 %module(package="test_package") test_module
131 %include "test.h"

```

132 The `%module` directive sets the name of the generated module and the package it will be located in and  
 133 the `%include` directive parses and automatically generates wrapper functions for the C++ header file. We  
 134 use SWIG in this manner to wrap both the model building and `SharedLibraryModel` APIs described in  
 135 section 2.1. However, key parts of GeNN’s API such as the `ModelSpec::addNeuronPopulation` method  
 136 employed in section 2.1, rely on C++ templates which are not directly translatable to Python. Instead, valid  
 137 template instantiations need to be given a unique name in Python using the `%template` SWIG directive:

```

138 %template(addNeuronPopulationLIF) ModelSpec::addNeuronPopulation<NeuronModels::LIF>;

```

139 Having to manually add these directives whenever a model is added to GeNN would be exactly the sort  
 140 of maintenance overhead we were trying to avoid by using SWIG. Therefore, when building the Python  
 141 wrapper, we instead search the GeNN header files for the macros used to declare models in C++ and  
 142 automatically generate SWIG `%template` directives.

143 As previously discussed, a key feature of GeNN is the ease with which it allows users to define their  
 144 own neuron and synapse models as well as ‘snippets’ defining how variables and connectivity should be  
 145 initialised. Beneath the syntactic sugar described in our previous work (Knight and Nowotny, 2018), new  
 146 models can be defined in C++ by defining a new class derived from, for example, the `NeuronModels::Base`  
 147 class. The ability to extend this system to Python was a key requirement of PyGeNN and, by using SWIG  
 148 ‘director’, C++ classes can be made inheritable from Python using a single SWIG directive:

```

149 %feature("director") NeuronModels::Base;

```

## 150 2.3 PyGeNN

151 While GeNN *could* be used from Python via the wrapper generated using SWIG, the resultant code  
 152 would be unpleasant to use directly. For example, rather than being able to specify neuron parameters  
 153 using a native Python types such as lists or dictionaries, one would have to use a wrapped type such as  
 154 `DoubleVector([0.25, 10.0, 0.0, 0.0, 20.0, 2.0, 0.5])`. Therefore, in order to provide a more  
 155 user-friendly and pythonic interface, we have built PyGeNN on top of the wrapper generated by SWIG.

PyGeNN combines the separate model building and simulation stages of building a GeNN model in C++ into a single API, likely to be more familiar to users of existing Python-based model description languages such as PyNEST (Eppler et al., 2009) or PyNN (Davison et al., 2008). By combining the two stages together, PyGeNN can provide a unified dictionary-based API for initialising homogeneous and heterogeneous parameters as shown in this re-implementation of the previous example:

```

161 from pygenn import genn_wrapper, genn_model
162
163 model = genn_model.GeNNModel("float", "izhikevich")
164 model.dT = 0.1
165
166 izk_init = {"V": -65.0,
167            "U": -20.0,
168            "a": [ 0.02, 0.1, 0.02, 0.02],
169            "b": [ 0.2, 0.2, 0.2, 0.2],
170            "c": [-65.0, -65.0, -50.0, -55.0],
171            "d": [ 8.0, 2.0, 2.0, 4.0]}
172
173 pop = model.add_neuron_population("Pop", 4, "IzhikevichVariable",
174                                 {}, izk_init)
175 model.add_current_source("CS", "DC", "Pop",
176                          {"amp": 10.0}, {})
177
178 model.build()
179 model.load()
180
181 v = pop.vars["V"].view
182 while model.t < 200.0:
183     model.step_time()
184     model.pull_state_from_device("Pop")
185     print("%f, %f, %f, %f, %f"
186           % (model.t, v[0], v[1], v[2], v[3]))

```

Initialisation of variables with homogeneous values – such as the neurons’ membrane potential – is performed by initialisation kernels generated by GeNN and initialisation of variables with heterogeneous values – such as the **a**, **b** and **c** parameters – are copied to the GPU by PyGeNN after the model is loaded. While the PyGeNN API is more pythonic and, hopefully, more user-friendly than the C++ interface, it still provides users with the same low-level control over the simulation. Furthermore, by using SWIG’s numpy (Van Der Walt et al., 2011) interface, the host memory allocated by GeNN can be accessed directly from Python using the `pop.vars["V"].view` syntax meaning that no potentially expensive additional copying of data is required.

As illustrated in the previously-defined model, for convenience, PyGeNN allows users to access GeNN’s built-in models. However, one of PyGeNN’s most powerful features is that it enables users to easily define their own neuron and synapse models from within Python. For example, an Izhikevich neuron model (Izhikevich, 2003) can be defined using the `create_custom_neuron_class` helper function which provides some syntactic sugar over directly inheriting from the SWIG director class:

```

200 izk_model = genn_model.create_custom_neuron_class(
201     "izk",

```



```

202 param_names=["a", "b", "c", "d"],
203 var_name_types=[("V", "scalar"), ("U", "scalar")],
204 sim_code=
205     """
206     $ (V) += 0.5 * (0.04 * $ (V) * $ (V) + 5.0 * $ (V) + 140.0 - $ (U) + $ (Isyn)) * DT;
207     $ (V) += 0.5 * (0.04 * $ (V) * $ (V) + 5.0 * $ (V) + 140.0 - $ (U) + $ (Isyn)) * DT;
208     $ (U) += $ (a) * ($ (b) * $ (V) - $ (U)) * DT;
209     """,
210 threshold_condition_code="$ (V) >= 30.0",
211 reset_code=
212     """
213     $ (V) = $ (c) ;
214     $ (U) += $ (d) ;
215     """)

```

216 The `param_names` list defines the real-valued parameters that are constant across the whole population of  
 217 neurons and the `var_name_types` list defines the model state variables and their type (the `scalar` type  
 218 is an alias for either single or double-precision floating point, depending on the precision passed to the  
 219 `GeNNModel` constructor). The behaviour of the model is then defined using a number of code strings. Unlike  
 220 in tools like Brian 2 (Stimberg et al., 2019), these code strings are specified in a C-like language rather than  
 221 using differential equations. This allows expert users to choose their own solver for models described in  
 222 terms of differential equations and to programatically define models such as spike sources. For example,  
 223 in the model presented above, we chose to implement the neuron using the idiosyncratic forward Euler  
 224 integration scheme employed by Izhikevich (2003). Finally, the `threshold_condition_code` expression  
 225 defines *when* the neuron will spike whereas the `reset_code` code string defines how the state variables  
 226 should be reset after a spike.

## 227 2.4 Spike recording system

228 Internally, GeNN stores the spikes emitted by a neuron population during one simulation timestep in  
 229 an array containing the indices of the neurons that spiked alongside a counter of how many spikes have  
 230 been emitted overall. Previously, recording spikes in GeNN was very similar to the recording of voltages  
 231 shown in the previous example code – the array of neuron indices was simply copied from the GPU to the  
 232 CPU every timestep. However, especially when simulating models with a small simulation timestep, such  
 233 frequent synchronization between the CPU and GPU is costly – especially if a slower, interpreted language  
 234 such as Python is involved. Furthermore, biological neurons typically spike at a low rate (in the cortex, the  
 235 average firing rate is only around 3 Hz (Buzsáki and Mizuseki, 2014)) meaning that the amount of spike  
 236 data transferred every timestep is typically very small. To address both of these sources of inefficiency,  
 237 we have added a new data structure to GeNN which stores spike data for many timesteps on the GPU. To  
 238 reduce the memory required for this data structure and to make its size independent of neural activity, the  
 239 spikes emitted by a population of  $N$  neurons in a single simulation timestep are stored in a  $N$ bit bitfield  
 240 where a ‘1’ represents a spike and a ‘0’ the absence of one. Spiking data over multiple timesteps is then  
 241 represented by a circular buffer of these bitfields. Using this approach, even the spiking output of relatively  
 242 large models, running for many timesteps can be stored in a small amount of memory. For example, the  
 243 spiking output of a model with  $100 \times 10^3$  neurons running for  $10 \times 10^3$  simulation timesteps, required  
 244 less than 120 MB – a small fraction of the memory on a modern GPU. While efficiently handling spikes  
 245 stored in a bitfield is a little trickier than working with a list of neuron indices, GeNN provides an efficient

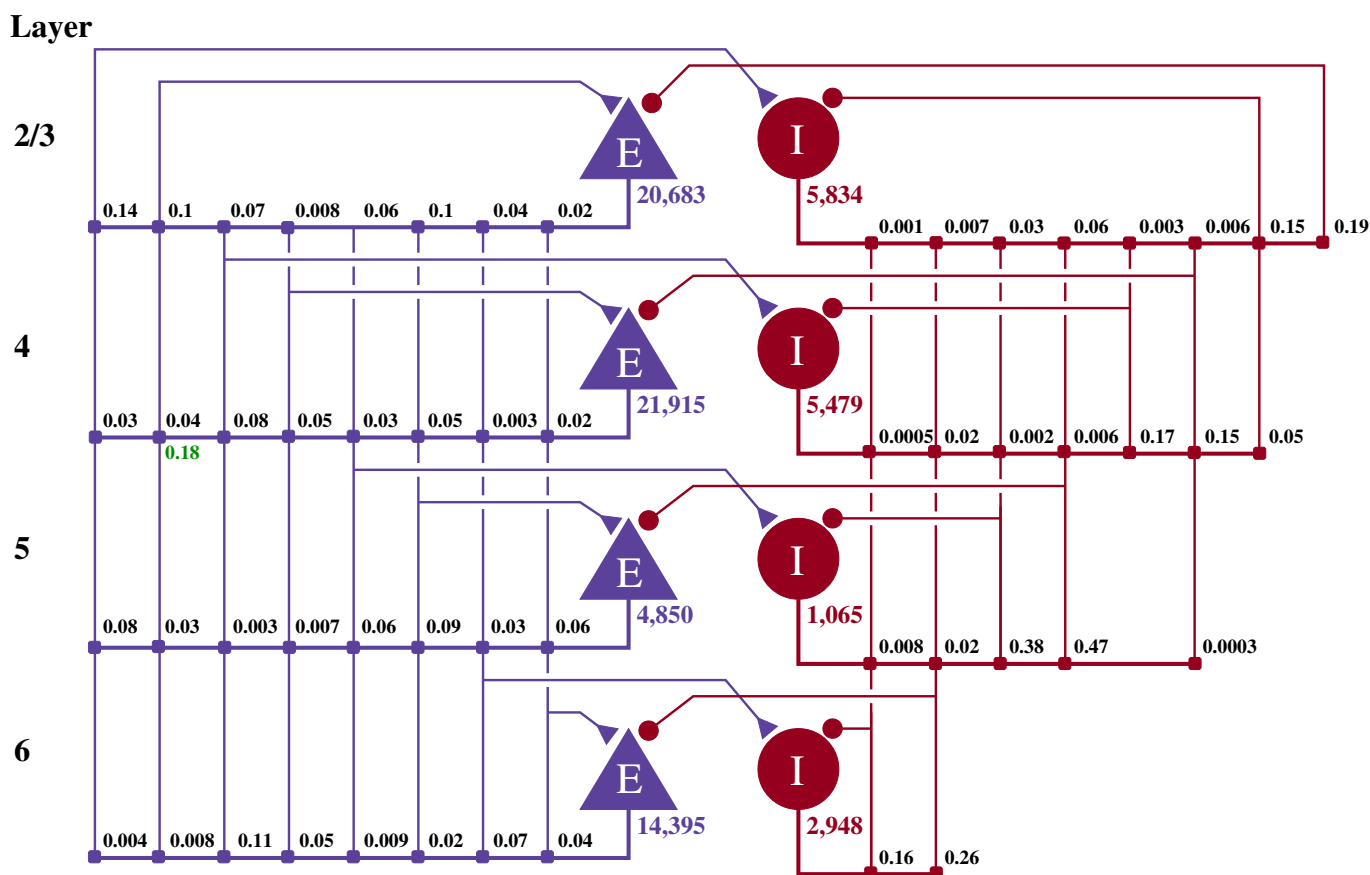


**Figure 1.** Illustration of the microcircuit model. Blue triangles represent excitatory populations, red circles represent inhibitory populations and the number beneath each symbol shows the number of neurons in each population. Connection probabilities are shown in small bold numbers at the appropriate point in the connection matrix. All excitatory synaptic weights are normally distributed with a mean of 0.0878 nA (unless otherwise indicated in green) and a standard deviation of 0.008 78 nA. All inhibitory synaptic weights are normally distributed with a mean of 0.3512 nA and a standard deviation of 0.035 12 nA.

246 C++ helper function for saving the spikes stored in a bitfield to a text file and a numpy-based method for  
 247 decoding them in PyGeNN.

## 248 2.5 Cortical microcircuit model

Potjans and Diesmann (2014) developed the cortical microcircuit model of 1 mm<sup>3</sup> of early-sensory cortex illustrated in figure 1. The model consists of 77 169 LIF neurons, divided into separate populations representing the excitatory and inhibitory population in each of 4 cortical layers (2/3, 4, 5 and 6). The membrane voltage  $V_i$  of each neuron  $i$  is modelled as:

$$\tau_m \frac{dV_i}{dt} = (V_{\text{rest}} - V_i) + R_m (I_{\text{syn}_i} + I_{\text{ext}_i}), \quad (1)$$

where  $\tau_m = 10$  ms and  $R_m = 40$  M $\Omega$  represent the time constant and resistance of the neuron's cell membrane,  $V_{\text{rest}} = -65$  mV defines the resting potential,  $I_{\text{syn}_i}$  represents the synaptic input current and  $I_{\text{ext}_i}$  represents an external input current. When the membrane voltage crosses a threshold  $V_{\text{th}} = -50$  mV a spike is emitted, the membrane voltage is reset to  $V_{\text{rest}}$  and updating of  $V$  is suspended for a refractory period  $\tau_{\text{ref}} = 2$  ms. Neurons in each population are connected randomly with numbers of synapses derived

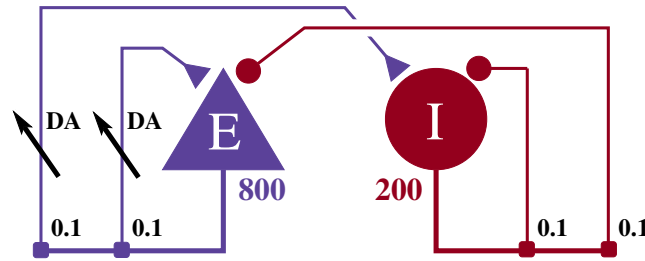


**Figure 2.** Illustration of the balanced random network model. The blue triangle represents the excitatory population, the red circle represents the inhibitory population, and the numbers beneath each symbol show the number of neurons in each population. Connection probabilities are shown in small bold numbers at the appropriate point in the connection matrix. All excitatory synaptic weights are plastic and initialised to 1 and all inhibitory synaptic weights are initialised to  $-1$ .

from an extensive review of the anatomical literature. These synapses are current-based, i.e. presynaptic spikes lead to exponentially-decaying input currents  $I_{\text{syn}_i}$

$$\tau_{\text{syn}} \frac{dI_{\text{syn}_i}}{dt} = -I_{\text{syn}_i} + \sum_{j=0}^n w_{ij} \sum_{t_j} \delta(t - t_j), \quad (2)$$

where  $\tau_{\text{syn}} = 0.5$  ms represents the synaptic time constant,  $w_{ij}$  represents the synaptic weight and  $t_j$  are the arrival times of incoming spikes from  $n$  presynaptic neurons. Within each synaptic projection, all synaptic strengths and transmission delays are normally distributed using the parameters presented in Potjans and Diesmann (2014, table 5) and, in total, the model has approximately  $0.3 \times 10^9$  synapses. As well as receiving synaptic input, each neuron in the network also receives an independent Poisson input current, representing input from neighbouring not explicitly modelled cortical regions. The Poisson input is delivered to each neuron via  $I_{\text{ext}_i}$  with

$$\tau_{\text{syn}} \frac{dI_{\text{ext}_i}}{dt} = -I_{\text{ext}_i} + w_{\text{ext}} \text{Poisson}(\nu_{\text{ext}} \Delta t), \quad (3)$$

where  $\nu_{\text{ext}}$  represents the mean input rate and  $w_{\text{ext}}$  represents the weight. The ordinary differential Eq. 1, (2) and (3) are solved with an exponential Euler algorithm. For a full description of the model parameters, please refer to Potjans and Diesmann (2014, tables 4 and 5) and for a description of the strategies used by GeNN to parallelise the initialisation and subsequent simulation of this network, please refer to Knight and Nowotny (2018, section 2.3). This model requires simulation using a relatively small timestep of 0.1 ms, making the overheads of copying spikes from the GPU every timestep particularly problematic.

## 2.6 Pavlovian conditioning model

The cortical microcircuit model described in the previous section is ideal for exploring the performance of short simulations of relatively large models. However, the performance of longer simulations of smaller models is equally vital. Such models can be particularly troublesome for GPU simulation as, not only might they not offer enough parallelism to fully occupy the device but, each timestep can be simulated so quickly that the overheads of launching kernels etc can dominate. Additional overheads can be incurred when models require injecting external stimuli throughout the simulation. Longer simulations are particularly useful when exploring synaptic plasticity so, to explore the performance of PyGeNN in this scenario, we



simulate a model of Pavlovian conditioning using a three-factor Spike-Timing-Dependent Plasticity (STDP) learning rule (Izhikevich, 2007).

## 2.6.1 Neuron model

The model illustrated in figure 2 consists of an 800 neuron excitatory population and a 200 neuron inhibitory population, within which, each neuron  $i$  is modelled using the Izhikevich model (Izhikevich, 2003) whose dimensionless membrane voltage  $V_i$  and adaption variables  $U_i$  evolve such that:

$$\frac{dV_i}{dt} = 0.04V_i^2 + 5V_i + 140 - U_i + I_{\text{syn}_i} + I_{\text{ext}_i} \quad (4)$$

$$\frac{dU_i}{dt} = a(bV_i - U_i) \quad (5)$$

When the membrane voltage rises above 30, a spike is emitted and  $V_i$  is reset to  $c$  and  $d$  is added to  $U_i$ . Excitatory neurons use the regular-spiking parameters (Izhikevich, 2003) where  $a = 0.02$ ,  $b = 0.2$ ,  $c = -65.0$ ,  $d = 8.0$  and inhibitory neurons use the fast-spiking parameters (Izhikevich, 2003) where  $a = 0.1$ ,  $b = 0.2$ ,  $c = -65.0$ ,  $d = 2.0$ . Again,  $I_{\text{syn}_i}$  represents the synaptic input current and  $I_{\text{ext}_i}$  represents an external input current. While there are numerous ways to solve Eq. 4 and 5 (Humphries and Gurney, 2007; Hopkins and Furber, 2015; Pauli et al., 2018), we chose to use the idiosyncratic forward Euler integration scheme employed by Izhikevich (2003) in the original work (Izhikevich, 2007). Under this scheme, Eq. 4 is first integrated for two 0.5 ms timesteps and then, based on the updated value of  $V_i$ , Eq. 5 is integrated for a single 1 ms timestep.

## 2.6.2 Synapse models

The excitatory and inhibitory neural populations are connected recurrently, as shown in figure 1, with instantaneous current-based synapses:

$$I_{\text{syn}_i}(t) = \sum_{j=0}^n w_{ij} \sum_{t_j} \delta(t - t_j), \quad (6)$$

where  $t_j$  are the arrival times of incoming spikes from  $n$  presynaptic neurons. Inhibitory synapses are static with  $w_{ij} = -1.0$  and excitatory synapses are plastic. Each plastic synapse has an eligibility trace  $C_{ij}$  as well as a synaptic weight  $w_{ij}$  and these evolve according to a three-factor STDP learning rule (Izhikevich, 2007):

$$\frac{dC_{ij}}{dt} = -\frac{C_{ij}}{\tau_c} + \text{STDP}(\Delta t)\delta(t - t_{\text{pre/post}}) \quad (7)$$

$$\frac{dw_{ij}}{dt} = -C_{ij}D_j \quad (8)$$

where  $\tau_c = 1000$  ms represents the decay time constant of the eligibility trace and  $\text{STDP}(\Delta t)$  describes the magnitude of changes made to the eligibility trace in response to the relative timing of a pair of pre and postsynaptic spikes with temporal difference  $\Delta t = t_{\text{post}} - t_{\text{pre}}$ . These changes are only applied to the trace at the times of pre and postsynaptic spikes as indicated by the Dirac delta function  $\delta(t - t_{\text{pre/post}})$ . Here, a

double exponential STDP kernel is employed such that:

$$\text{STDP}(\Delta t) = \begin{cases} A_+ \exp\left(-\frac{\Delta t}{\tau_+}\right) & \text{if } \Delta t > 0 \\ A_- \exp\left(\frac{\Delta t}{\tau_-}\right) & \text{if } \Delta t < 0 \\ 0 & \text{otherwise} \end{cases} \quad (9)$$

where the time constant of the STDP window  $\tau_+ = \tau_- = 20$  ms and the strength of potentiation and depression are  $A_+ = 0.1$  and  $A_- = 0.15$  respectively. Finally, each excitatory neuron has an additional variable  $D_j$  which describes extracellular dopamine concentration:

$$\frac{D_j}{t} = -\frac{D_j}{\tau_d} + \text{DA}(t) \quad (10)$$

277 where  $\tau_d = 200$  ms represents the time constant of dopamine uptake and  $\text{DA}(t)$  the dopamine input over  
278 time.

### 279 2.6.3 PyGeNN implementation of three-factor STDP

280 The first step in implementing this learning rule in PyGeNN is to implement the STDP updates and decay  
281 of  $C_{ij}$  using GeNN's event-driven plasticity system, the implementation of which was described in our  
282 previous work (Knight and Nowotny, 2018). Using a similar syntax to that described in section 2.3, we first  
283 create a new 'weight update model' with the learning rule parameters and the  $w_{ij}$  and  $C_{ij}$  state variables:

```
284 izhikevich_stdp_model = create_custom_weight_update_class(
285     "izhikevich_stdp",
286
287     param_names=["tauPlus", "tauMinus",
288                 "tauC", "aPlus", "aMinus"],
289     var_name_types=[("w", "scalar"), ("c", "scalar")],
```

290 We then instruct GeNN to record the times of current and previous pre and postsynaptic spikes. **(TODO:**  
291 **IMPROVE SENTENCE)** The current spike time will equal the current time if a spike of this sort is being  
292 processed in the current timestep whereas the previous spike time only tracks spikes which have occurred  
293 *before* the current timestep:

```
294     is_pre_spike_time_required=True,
295     is_post_spike_time_required=True,
296
297     is_prev_pre_spike_time_required=True,
298     is_prev_post_spike_time_required=True,
```

299 Next we define the 'sim code' which is called whenever presynaptic spikes arrive at the synapse. This code  
300 first implements Eq. 6 – adding the synaptic weight ( $w_{ij}$ ) to the postsynaptic neuron's input ( $I_{\text{syn}_i}$ ) using  
301 the `$ (addToInSyn, x)` function.

```
302     sim_code=
303         """
304         $ (addToInSyn, $ (w)) ;
```

305 Within the sim code we also need to calculate the time that has elapsed since the last update of  $C_{ij}$  using  
 306 the spike times we previously requested that GeNN record. Within a timestep, GeNN processes presynaptic  
 307 spikes before postsynaptic spikes so the time of the last update to  $C_{ij}$  will be the latest time either type of  
 308 spike was processed in previous timesteps:

```
309         const scalar tc = fmax($(prev_sT_pre),
310                                $(prev_sT_post));
```

311 Using this time, we can now calculate how much to decay  $C_{ij}$  using the closed-form solution to Eq. 7:

```
312         const scalar tagDecay = exp(-$(t) - tc) / $(tauC);
313         scalar newTag = $(c) * tagDecay;
```

314 To complete the sim code we calculate the depression case of Eq. 9 (here we use the *current* postsynaptic  
 315 spike time as, if a postsynaptic and presynaptic spike occur in the same timestep, there should be no  
 316 update).

```
317         const scalar dt = $(t) - $(sT_post);
318         if (dt > 0) {
319             newTag -= ($(aMinus) * exp(-dt / $(tauMinus)));
320         }
321         $(c) = newTag;
322         """,
```

323 Finally we define the ‘learn post code’ which is called whenever a postsynaptic spike arrives at the synapse.  
 324 Other than implementing the potentiation case of Eq. 9 and using the *current* presynaptic spike time when  
 325 calculating the time since the last update of  $C_{ij}$  – in order to correctly handle presynaptic updates made in  
 326 the same timestep – this code is very similar to the sim code:

```
327     learn_post_code=
328         """
329         const scalar tc = fmax($(sT_pre),
330                                $(prev_sT_post));
331
332         const scalar tagDecay = exp(-$(t) - tc) / $(tauC);
333         scalar newTag = $(c) * tagDecay;
334
335         const scalar dt = $(t) - $(sT_pre);
336         if (dt > 0) {
337             newTag += ($(aPlus) * exp(-dt / $(tauPlus)));
338         }
339         $(c) = newTag;
340         """)
```

341 Adding the synaptic weight  $w_{ij}$  update described by Eq. 8 requires two further additions to the model.  
 342 As well as the pre and postsynaptic spikes, the weight update model needs to receive events whenever  
 343 dopamine is injected via DA. GeNN supports such events via the ‘spike-like event’ system which allows  
 344 events to be triggered based on an expression evaluated on the presynaptic neuron. In this case, this  
 345 expression simply tests an `injectDopamine` flag which gets set by the dopamine injection logic in our  
 346 presynaptic neuron model:

```

347     event_threshold_condition_code="injectDopamine",

348 In order to extend our event-driven update of  $C_{ij}$  to include spike-like events we need to instruct GeNN to
349 record the times at which they occur:

350     is_pre_spike_event_time_required=True,
351     is_prev_pre_spike_event_time_required=True,

352 The spike-like events can now be handled using a final ‘event code’ string:

353     event_code=
354         """
355         const scalar tc = fmax($(sT_pre), fmax($(prev_sT_post), $(prev_seT_pre)));
356         const scalar tagDecay = exp(-$(t) - tc) / $(tauC));
357         $(c) *= tagDecay;
358         """,

```

After updating the previously defined calculations of `tc` in the sim code and learn post code in the same way to also include the times of spike-like events, all that remains is to update  $w_{ij}$ . Mikaitis et al. (2018) showed how Eq. 8 could be solved algebraically, allowing  $w_{ij}$  to be updated in an event-driven manner with:

$$\Delta w_{ij} = \frac{C(t_c^{last})D(t_d^{last})}{-\left(\frac{1}{\tau_c} + \frac{1}{\tau_d}\right)} \left( e^{-\frac{t-t_c^{last}}{\tau_c}} e^{-\frac{t-t_d^{last}}{\tau_d}} - e^{-\frac{t_w^{last}-t_c^{last}}{\tau_c}} e^{-\frac{t_w^{last}-t_d^{last}}{\tau_d}} \right) \quad (11)$$

where  $t_c^{last}$ ,  $t_w^{last}$  and  $t_d^{last}$  represent the last times at which  $C_{ij}$ ,  $W_{ij}$  and  $D_j$  respectively were updated. Because we will always update  $w_{ij}$  and  $C_{ij}$  together when presynaptic, postsynaptic and spike-like events occur,  $t_c^{last} = t_w^{last}$  and Eq. 11 can be simplified to:

$$\Delta w_{ij} = \frac{C(t_c^{last})D(t_d^{last})}{-\left(\frac{1}{\tau_c} + \frac{1}{\tau_d}\right)} \left( e^{-\frac{t-t_c^{last}}{\tau_c}} e^{-\frac{t-t_d^{last}}{\tau_d}} - e^{-\frac{t_c^{last}-t_d^{last}}{\tau_d}} \right) \quad (12)$$

```

359 and this update can now be added to each of our three event handling code strings to complete the
360 implementation of the learning rule.

```

#### 361 2.6.4 PyGeNN implementation of Pavlovian conditioning experiment

```

362 To perform the Pavlovian conditioning experiment described by Izhikevich (2007) using this model, we
363 chose 100 random groups of 50 neurons (each representing stimuli  $S_1 \dots S_{100}$ ) from amongst the two neural
364 populations. Stimuli are presented to the network in a random order, separated by intervals sampled from
365  $U(100, 300)$ ms. The neurons associated with an active stimulus are stimulated for a single 1 ms simulation
366 timestep with a current of 40.0 nA, in addition to the random background current of  $U(-6.5, 6.5)$ nA,
367 delivered to each neuron via  $I_{ext_i}$  throughout the simulation.  $S_1$  is arbitrarily chosen as the Conditional
368 Stimuli (CS) and, whenever this stimuli is presented, a reward in the form of an increase in dopamine
369 is delivered by setting  $DA(t) = 0.5$  after a delay sampled from  $U(0, 1000)$ ms. This delay period is large
370 enough to allow a few irrelevant stimuli to be presented which act as distractors. The simplest way to
371 implement this stimulation regime is to add a current source to the excitatory and inhibitory neuron

```

populations which adds the uniformly-distributed input current to an externally-controllable per-neuron current. In PyGeNN, the following model can be defined to do just that:

```

374 stim_noise_model = create_custom_current_source_class(
375     "stim_noise",
376     param_names=["n"],
377     var_name_types=[("iExt", "scalar", VarAccess_READ_ONLY)],
378     injection_code=
379         """
380         $(injectCurrent, $(iExt) + ($(gennrand_uniform) * $(n) * 2.0) - $(n));
381         """

```

where the `n` parameter sets the magnitude of the background noise, the `$(injectCurrent, I)` function injects a current of  $I$  nA into the neuron and `$(gennrand_uniform)` samples from  $U(0, 1)$  using the ‘XORWOW’ pseudo-random number generator provided by cuRAND (NVIDIA Corporation, 2019). Once a current source population using this model has been instantiated and a memory view to `iExt` obtained in the manner described in section 2.3, in timesteps when stimulus injection is required, current can be injected into the list of neurons contained in `stimuli_input_set` with:

```

388 curr_ext_view[stimuli_input_set] = 40.0
389 curr_pop.push_var_to_device("iExt")

```

The same approach can then be used to zero the current afterwards. However, as almost 20 000 stimuli will be injected over the course of a 1 h simulation, we can offload the stimulus delivery entirely to the GPU in order to reduce potential overheads, using the following slightly more complex model:

```

393 stim_noise_model = create_custom_current_source_class(
394     "stim_noise",
395     param_names=["n", "stimMagnitude"],
396     var_name_types=[("startStim", "unsigned int"),
397                     ("endStim", "unsigned int", VarAccess_READ_ONLY)],
398     extra_global_params=[("stimTimes", "scalar*")],
399     injection_code=
400         """
401         scalar current = ($(gennrand_uniform) * $(n) * 2.0) - $(n);
402         if($(startStim) != $(endStim) && $(t) >= $(stimTimes)[$(startStim)]) {
403             current += $(stimMagnitude);
404             $(startStim)++;
405         }
406         $(injectCurrent, current);
407         """

```

This model retains the same logic for generating background noise but adds a `stimTimes` array which contains the times at which each neuron should have current injected. This array is an ‘extra global parameter’ – a read-only memory area that can be allocated and populated from PyGeNN, in this case by ‘stacking’ together a list of lists of spike times:

```

412 curr_pop.set_extra_global_param("stimTimes", np.hstack(neuron_stimuli_times))

```

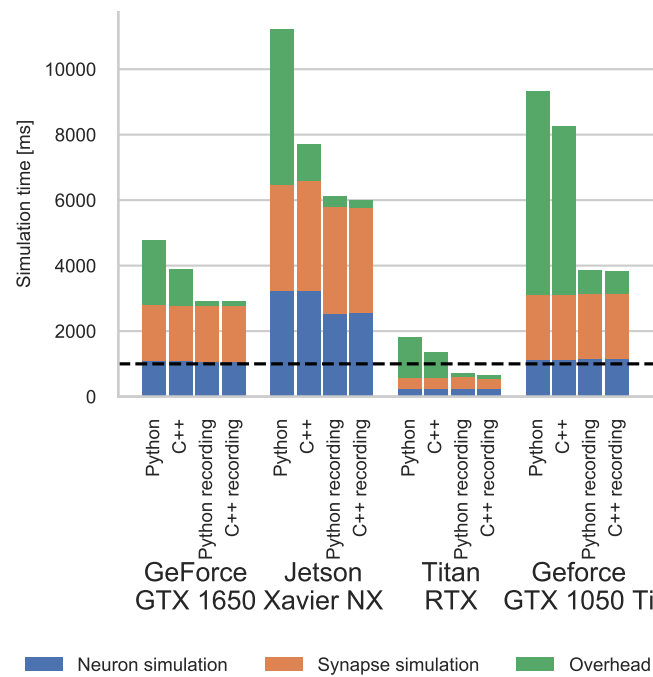


**Figure 3.** Simulation times of the microcircuit model running on various GPU hardware for 1 s of biological time. ‘Overhead’ refers to time spent in simulation loop but not within CUDA kernels. The dashed horizontal line indicates realtime performance

413 The `startStim` and `endStim` variables are then used to point to the subset of the `stimTimes` array  
 414 corresponding to each neuron. Once the simulation time (`$t`) passes the time at `stimTimes[startStim]`,  
 415 current is injected and `startStim` is advanced.

### 3 RESULTS

416 In the following subsections we will analyse the performance of the models introduced in  
 417 sections 2.5 and 2.6 on a representative selection of NVIDIA GPU hardware:

- 418 • Jetson Xavier NX – a low-power embedded system with a GPU based on the Volta architecture with  
 419 8 GB of shared memory.
- 420 • GeForce GTX 1050Ti – a low-end desktop GPU based on the Pascal architecture with 4 GB of  
 421 dedicated memory.
- 422 • GeForce GTX 1650 – a low-end desktop GPU based on the Turing architecture with 4 GB of dedicated  
 423 memory.
- 424 • Titan RTX – a high-end workstation GPU based on the Turing architecture with 24 GB of dedicated  
 425 memory.

426 All of these systems run Ubuntu 18 apart from the system with the GeForce 1050 Ti which runs Windows  
 427 10.

#### 3.1 Cortical microcircuit model performance

429 Figure 3 shows the simulation times for the full-scale microcircuit model. We measured the  
 430 total simulation time by querying the `std::chrono::high_resolution_clock` in C++ and the



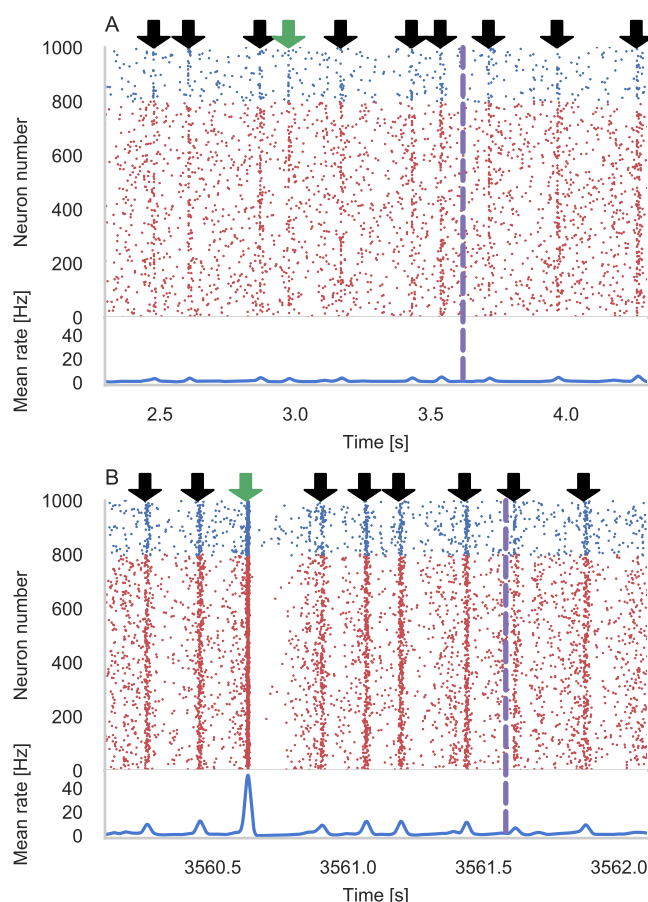


**Figure 4.** Results of Pavlovian conditioning experiment. Raster plot and spike density function (SDF) (Szücs, 1998) showing activity centred around first delivery of Conditional Stimulus (CS) during initial (A) and final (B) 50 s of simulation. Downward green arrows indicate times at which CS is delivered and downward black arrows indicate times when other, un-rewarded stimuli are delivered. Vertical dashed lines indicate times at which dopamine is delivered. The population SDF was calculated by convolving the spikes with a Gaussian kernel of  $\sigma = 10$  ms width.

431 `time.perf_counter` in Python before and after the simulation loop; and used CUDA's own event timing  
 432 system (NVIDIA Corporation, 2021, Section 3.2.6.7) to record the time taken by the neuron and synapse  
 433 kernels. As one might predict, the Jetson Xavier NX is slower than the three desktop GPUs but, considering  
 434 that it only consumes a maximum of 15 W compared to 75 W or 320 W for the GeForce cards and Titan  
 435 RTX respectively, it still performs impressively. The time taken to actually simulate the models ('Neuron  
 436 simulation' and 'Synapse simulation') are the same when using Python and C++ as all GeNN optimisation  
 437 options are exposed to PyGeNN. Interestingly, when simulating *this* model, the larger L1 cache and  
 438 architectural improvements present in the Turing-based GTX 1650 do not result in significantly improved  
 439 performance over the Pascal-based GTX 1050Ti. Instead, the slightly improved performance of the GTX  
 440 1650 can probably be explained by its additional 128 CUDA cores.

441 Without the recording system described in section 2.4, the CPU and GPU need to be synchronised  
 442 after every timestep to allow spike data to be copied off the GPU and stored in a suitable data structure.  
 443 The 'overheads' shown in figure 3 indicate the time taken by these processes as well as the unavoidable  
 444 overheads of launching CUDA kernels etc. Because Python is an interpreted language, updating the spike  
 445 data structures is somewhat slower and this is particularly noticeable on devices with a slower CPU such

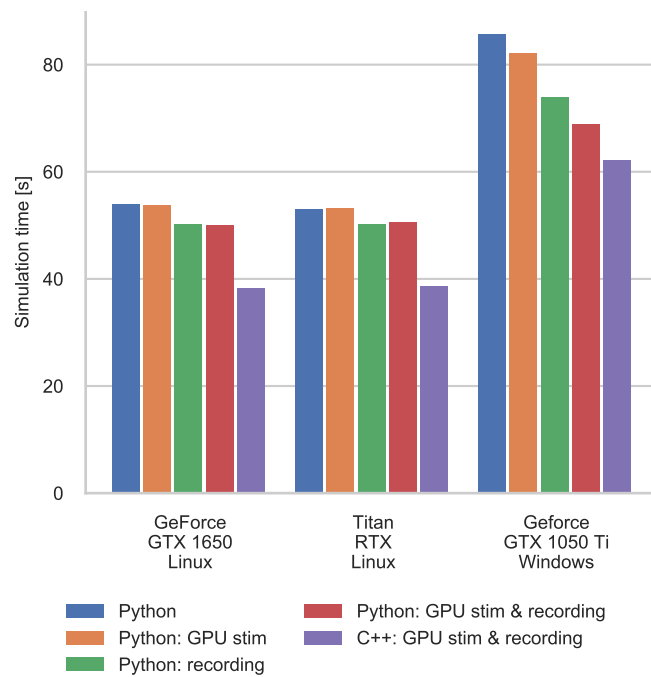


**Figure 5.** Simulation times of the Pavlovian Conditioning model running on various GPU hardware for 1 h of biological time. ‘GPU stim’ indicates simulations using the GPU stimulus delivery model and ‘recording’ indicates simulations where the new recording system is employed.

as the Jetson Xavier NX. However, unlike the desktop GPUs, the Jetson Xavier NX’s 8 GB of memory is shared between the GPU and the CPU meaning that data does not need to be copied between their memories and can instead be accessed by both. While, using this shared memory for recording spikes reduces the overhead of copying data off the device, because the GPU and CPU caches are not coherent, caching must be disabled on this memory which reduces the performance of the neuron kernel. Although the Windows machine has a relatively powerful CPU, the overheads measured in both the Python and C++ simulations run on this system are extremely large due to additional queuing between the application and the GPU driver caused by the Windows Display Driver Model (WDDM). When small – in this case 0.1 ms – simulation timesteps are used, this makes per-timestep synchronisation disproportionately expensive.

However, when the spike recording system described in section 2.4 is used, spike data is kept in GPU memory until the end of the simulation and overheads are reduced by up to 10×. Because synchronisation with the CPU is no longer required every timestep, simulations run approximately twice as fast on the Windows machine. Furthermore, on the high-end desktop GPU, the simulation now runs faster than real-time in both Python and native C++ versions – significantly faster than other recently published GPU simulators (Golosio et al., 2020) and even specialised neuromorphic systems (Rhodes et al., 2020).

### 3.2 Pavlovian conditioning performance

Figure 4 shows the results of an example simulation of the Pavlovian conditioning model. At the beginning of each simulation (Figure 4A), the neurons representing every stimulus respond equally. However, after 1 h of simulation, the response to the CS becomes much stronger (Figure 4B) – showing that these neurons have been selectively associated with the stimulus even in the presence of the distractors and the delayed reward.

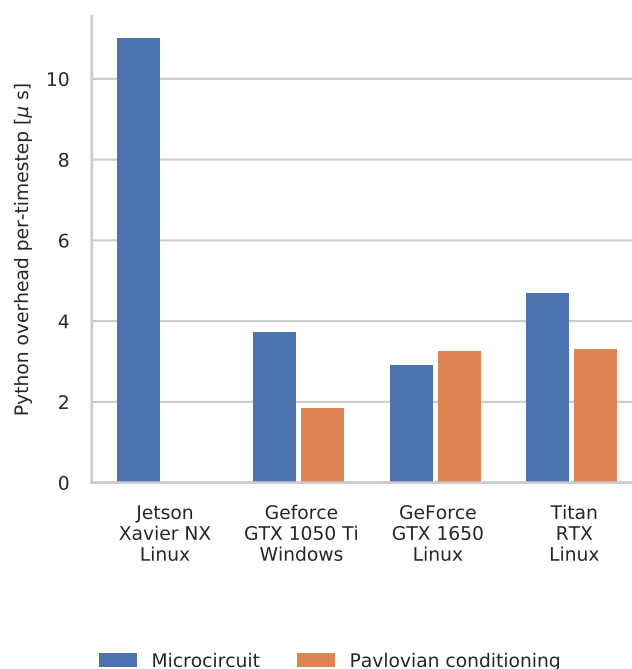


**Figure 6.** Comparison of the duration of individual timestep in Python and C++ simulation in microcircuit and Pavlovian conditioning experiments. Times are taken from the fastest version of each model i.e. the microcircuit using the recording system and the Pavlovian conditioning model using the recording system and the GPU stimulus delivery.

467 In figure 5, we show the runtime performance of simulations of the Pavlovian conditioning model,  
 468 running on a selection of desktop GPUs using PyGeNN with and without the recording system described  
 469 in section 2.4 and the optimized stimulus-delivery described in section 2.6. These PyGeNN results are  
 470 compared to a C++ simulation using both optimizations. Because each simulation timestep only takes  
 471 a few  $\mu$ s, the overhead of using CUDA timing events significantly alters the performance so, for this  
 472 model, we only measure the duration of the simulation loop using the approaches described in the previous  
 473 section. Interestingly the Titan RTX and GTX 1650 perform identically in this benchmark with speedups  
 474 ranging from  $62\times$  to  $72\times$  real-time. This is because, as discussed previously, this model is simply not  
 475 large enough to fill the 4608 CUDA cores present on the Titan RTX. Therefore, as the two GPUs share  
 476 the same Turing architecture and have very similar clock speeds (1350 MHz–1770 MHz for the Titan RTX  
 477 and 1485 MHz–1665 MHz for the GTX 1650), the two GPUs perform very similarly. Although we only  
 478 record the spiking activity during the first and last 50 s, using the recording system on these two systems  
 479 still significantly improves the overall performance whereas, delivering stimuli on the GPU only provides  
 480 a minimal improvement. However, unlike in the simulations of the microcircuit model, here the GTX  
 481 1050 Ti performs rather differently. Although the clock speed of this device is approximately the same  
 482 as the other GPUs (1290 MHz–1392 MHz) and it has a similar number of CUDA cores to the GTX 1650,  
 483 its performance is significantly worse. The difference in performance across all configurations is likely  
 484 to be due to architectural differences between the older Pascal; and newer Volta and Turing architectures.  
 485 Specifically, Pascal GPUs have one type of Arithmetic Logic Unit (ALU) which handles both integer  
 486 and floating point arithmetic whereas, the newer Volta and Turing architectures have equal numbers of  
 487 dedicated integer and floating point ALUs as well as significantly larger L1 caches. As discussed in our  
 488 previous work (Knight and Nowotny, 2018), these architectural features are particularly beneficial for

SNN simulations with STDP where a large amount of floating point computation is required to update the synaptic state *and* additional integer arithmetic is required to calculate the indices into the sparse matrix data structures. Furthermore, due to the additional synchronisation overheads caused by the Windows Display Driver Model (WDDM) which we discussed in the previous section, offloading stimulus delivery to the GPU improves the performance significantly on the Windows machine.

The difference between the speeds of the Python and C++ simulations of the Pavlovian conditioning model (figure 5) *appear* much larger than those of the microcircuit model (figure 3). However, as figure 6 illustrates, for individual timesteps the excess time due to overheads is approximately the same for both models and consistent with the cost of a small number of Python to C++ function calls (Apache Crail, 2019). Depending on the size and complexity of the model as well as the hardware used, this overhead may or may not be important. For example, when simulating the microcircuit model for 1 s on the Titan RTX, the overhead of using Python is less than 0.2 % but, when simulating the Pavlovian conditioning model on the same device, the overhead of using Python is almost 31 %.

## 4 DISCUSSION

In this paper we have introduced PyGeNN, a Python interface to the C++ based GeNN library for GPU accelerated spiking neural network simulations.

Uniquely, the new interface provides access to all the features of GeNN, without leaving the comparative simplicity of Python and with, as we have shown, typically negligible overheads from the Python bindings. PyGeNN also allows bespoke neuron and synapse models to be defined from within Python, making PyGeNN much more flexible and broadly applicable than, for instance, the Python interface to NEST (Eppler et al., 2009) or the PyNN model description language used to expose CARLsim to Python (Balaji et al., 2020).

In many ways, the new interface resembles elements of the Python-based Brian 2 simulator (Stimberg et al., 2019) (and it's Brian2GeNN backend (Stimberg et al., 2020)) with two key differences. Unlike in Brian 2, bespoke models in PyGeNN are defined with 'C-like' code snippets. This has the advantage of unparalleled flexibility for the expert user, but comes at the cost of more complexity as the code for a timestep update needs to include a suitable solver as well as merely differential equations. The second difference lies in how data structures are handled. Whereas simulations run using the C++ or Brian2GeNN Brian 2 backends use files to exchange data with Python, the underlying GeNN data structures are directly accessible from PyGeNN meaning that no disk access is involved.

As we have demonstrated, the PyGeNN wrapper, exactly like native GeNN, can be used on a variety of hardware from data centre scale down to mobile devices such as the NVIDIA Jetson. This allows for the same codes to be used in large-scale brain simulations and embedded and embodied spiking neural network research. Supporting the popular Python language in this interface makes this ecosystem available to a wider audience of researchers in both Computational Neuroscience, bio-mimetic machine learning and autonomous robotics.

The new interface also opens up opportunities to support researchers that work with other Python based systems. In the Computational Neuroscience and Neuromorphic computing communities, we can now build a PyNN (Davison et al., 2008) interface on top of PyGeNN and, infact, a prototype of such an interface is in development. Furthermore, for the burgeoning spike-based machine learning community, we can use PyGeNN as the basis for a spike-based machine learning framework akin to TensorFlow or PyTorch for rate-based models. A prototype interface of this sort called mlGeNN is in development and close to release.

530 In this work we have introduced a new spike recording system for GeNN and have shown that, using  
531 this system, we can now simulate the Potjans microcircuit model (Potjans and Diesmann, 2014) faster  
532 than real-time and, to the best of our knowledge, faster than any other systems. Finally, the excellent  
533 performance we have demonstrated using low-end Turing architecture GPUs is very exciting in terms of  
534 increasing the accessibility of GPU accelerated Computational Neuroscience and SNN machine learning  
535 research.

## CONFLICT OF INTEREST STATEMENT

536 The authors declare that the research was conducted in the absence of any commercial or financial  
537 relationships that could be construed as a potential conflict of interest.

## AUTHOR CONTRIBUTIONS

538 JK and TN wrote the paper. TN is the original developer of GeNN. AK was the original developer of  
539 PyGeNN. JK is currently the primary developer of both GeNN and PyGeNN and was responsible for  
540 implementing the spike recording system. JK performed the experiments and the analysis of the results that  
541 are presented in this work.

## FUNDING

542 This work was funded by the EPSRC (Brains on Board project, grant number EP/P006094/1), the European  
543 Union's Horizon 2020 research and innovation program under Grant Agreement 945539 (HBP SGA3) and  
544 a Google Summer of Code grant to AK .

## ACKNOWLEDGMENTS

545 We would like to thank Malin Sandström and everyone else at the International Neuroinformatics  
546 Coordinating Facility (INCF) for their hard work running the Google Summer of Code mentoring  
547 organisation every year. Without them, this and many other exciting Neuroinformatics projects would not  
548 be possible.

## DATA AVAILABILITY STATEMENT

549 All models, data and analysis scripts used for this study can be found in [https://github.com/](https://github.com/BrainsOnBoard/pygenn_paper)  
550 [BrainsOnBoard/pygenn\\_paper](https://github.com/BrainsOnBoard/pygenn_paper).

## REFERENCES

- 551 Akar, N. A., Cumming, B., Karakasis, V., Kusters, A., Klijn, W., Peyser, A., et al. (2019). Arbor — A  
552 Morphologically-Detailed Neural Network Simulation Library for Contemporary High-Performance  
553 Computing Architectures. In *2019 27th Euromicro International Conference on Parallel, Distributed  
554 and Network-Based Processing (PDP)* (IEEE), 274–282. doi:10.1109/EMPDP.2019.8671560  
555 [Dataset] Apache Crail (2019). Crail Python API: Python -> C/C++ call overhead  
556 Balaji, A., Adiraju, P., Kashyap, H. J., Das, A., Krichmar, J. L., Dutt, N. D., et al. (2020). PyCARL: A  
557 PyNN Interface for Hardware-Software Co-Simulation of Spiking Neural Network



- 558 Beazley, D. M. (1996). Using SWIG to control, prototype, and debug C programs with Python. In *Proc.*  
 559 *4th Int. Python Conf*
- 560 Buzsáki, G. and Mizuseki, K. (2014). The log-dynamic brain: how skewed distributions affect network  
 561 operations. *Nature reviews. Neuroscience* 15, 264–78. doi:10.1038/nrn3687
- 562 Carnevale, N. T. and Hines, M. L. (2006). *The NEURON book* (Cambridge University Press)
- 563 Chou, T.-s., Kashyap, H. J., Xing, J., Listopad, S., Rounds, E. L., Beyeler, M., et al. (2018). CARLsim 4:  
 564 An Open Source Library for Large Scale, Biologically Detailed Spiking Neural Network Simulation  
 565 using Heterogeneous Clusters. In *2018 International Joint Conference on Neural Networks (IJCNN)*  
 566 (IEEE), 1–8. doi:10.1109/IJCNN.2018.8489326
- 567 Davison, A. P., Brüderle, D., Eppler, J., Kremkow, J., Müller, E., Pecevski, D., et al. (2008). PyNN: A  
 568 Common Interface for Neuronal Network Simulators. *Frontiers in neuroinformatics* 2, 11. doi:10.3389/  
 569 neuro.11.011.2008
- 570 Eppler, J. M., Helias, M., Müller, E., Diesmann, M., and Gewaltig, M. O. (2009). PyNEST: A convenient  
 571 interface to the NEST simulator. *Frontiers in Neuroinformatics* 2, 1–12. doi:10.3389/neuro.11.012.2008
- 572 Gewaltig, M.-O. and Diesmann, M. (2007). NEST (NEural Simulation Tool). *Scholarpedia* 2, 1430
- 573 Givon, L. E. and Lazar, A. A. (2016). Neurokernel: An open source platform for emulating the fruit fly  
 574 brain. *PLOS ONE* 11, 1–25. doi:10.1371/journal.pone.0146581
- 575 Golosio, B., Tiddia, G., De Luca, C., Pastorelli, E., Simula, F., and Paolucci, P. S. (2020). A new GPU  
 576 library for fast simulation of large-scale networks of spiking neurons , 1–27
- 577 Hines, M. L., Davison, A. P., and Müller, E. (2009). NEURON and Python. *Frontiers in Neuroinformatics*  
 578 3, 1–12. doi:10.3389/neuro.11.001.2009
- 579 Hopkins, M. and Furber, S. B. (2015). Accuracy and Efficiency in Fixed-Point Neural ODE Solvers.  
 580 *Neural computation* 27, 2148–2182
- 581 Humphries, M. D. and Gurney, K. (2007). Solution Methods for a New Class of Simple Model Neurons M.  
 582 *Neural Computation* 19, 3216–3225. doi:doi:10.1162/neco.2007.19.12.3216
- 583 Hunter, J. D. (2007). Matplotlib: A 2D graphics environment. *Computing in Science & Engineering* 9,  
 584 90–95. doi:10.1109/MCSE.2007.55
- 585 Izhikevich, E. M. (2003). Simple model of spiking neurons. *IEEE Transactions on neural networks* 14,  
 586 1569–72. doi:10.1109/TNN.2003.820440
- 587 Izhikevich, E. M. (2007). Solving the Distal Reward Problem through Linkage of STDP and Dopamine  
 588 Signaling. *Cerebral Cortex* 17, 2443–2452. doi:10.1093/cercor/bhl152
- 589 Knight, J. C. and Nowotny, T. (2018). GPUs Outperform Current HPC and Neuromorphic Solutions  
 590 in Terms of Speed and Energy When Simulating a Highly-Connected Cortical Model. *Frontiers in*  
 591 *Neuroscience* 12, 1–19. doi:10.3389/fnins.2018.00941
- 592 Knight, J. C. and Nowotny, T. (2020). Larger GPU-accelerated brain simulations with procedural  
 593 connectivity. *bioRxiv* doi:10.1101/2020.04.27.063693
- 594 Mikaitis, M., Pineda García, G., Knight, J. C., and Furber, S. B. (2018). Neuromodulated Synaptic  
 595 Plasticity on the SpiNNaker Neuromorphic System 12, 1–13. doi:10.3389/fnins.2018.00105
- 596 Millman, K. J. and Aivazis, M. (2011). Python for scientists and engineers. *Computing in Science and*  
 597 *Engineering* 13, 9–12. doi:10.1109/MCSE.2011.36
- 598 NVIDIA, Vingelmann, P., and Fitzek, F. H. (2020). *CUDA, developer.nvidia.com/cuda-toolkit*
- 599 NVIDIA Corporation (2019). *cuRAND Library, docs.nvidia.com/cuda/pdf/CURAND\_Library.pdf*
- 600 NVIDIA Corporation (2021). *CUDA C Programming Guide,*  
 601 *docs.nvidia.com/cuda/pdf/CUDA\_C\_Programming\_Guide.pdf*



- 602 Pauli, R., Weidel, P., Kunkel, S., and Morrison, A. (2018). Reproducing Polychronization: A Guide to  
603 Maximizing the Reproducibility of Spiking Network Models. *Frontiers in Neuroinformatics* 12, 1–21.  
604 doi:10.3389/fninf.2018.00046
- 605 Potjans, T. C. and Diesmann, M. (2014). The Cell-Type Specific Cortical Microcircuit: Relating Structure  
606 and Activity in a Full-Scale Spiking Network Model. *Cerebral Cortex* 24, 785–806. doi:10.1093/cercor/  
607 bhs358
- 608 Rhodes, O., Peres, L., Rowley, A. G. D., Gait, A., Plana, L. A., Brenninkmeijer, C., et al. (2020). Real-time  
609 cortical simulation on neuromorphic hardware. *Philosophical Transactions of the Royal Society A:  
610 Mathematical, Physical and Engineering Sciences* 378, 20190160. doi:10.1098/rsta.2019.0160
- 611 Stimberg, M., Brette, R., and Goodman, D. F. (2019). Brian 2, an intuitive and efficient neural simulator.  
612 *eLife* 8, 1–41. doi:10.7554/eLife.47314
- 613 Stimberg, M., Goodman, D. F., and Nowotny, T. (2020). Brian2GeNN: accelerating spiking neural network  
614 simulations with graphics hardware. *Scientific Reports* 10, 1–12. doi:10.1038/s41598-019-54957-7
- 615 Szücs, A. (1998). Applications of the spike density function in analysis of neuronal firing patterns. *J*  
616 *Neurosci Methods* 81, 159–167
- 617 Van Der Walt, S., Colbert, S. C., and Varoquaux, G. (2011). The NumPy array: A structure for efficient  
618 numerical computation. *Computing in Science and Engineering* 13, 22–30. doi:10.1109/MCSE.2011.37
- 619 Vitay, J., Dinkelbach, H., and Hamker, F. (2015). ANNarchy: a code generation approach to neural  
620 simulations on parallel hardware. *Frontiers in Neuroinformatics* 9, 19. doi:10.3389/fninf.2015.00019
- 621 Yavuz, E., Turner, J., and Nowotny, T. (2016). GeNN: a code generation framework for accelerated brain  
622 simulations. *Scientific reports* 6, 18854. doi:10.1038/srep18854